

## **(Al,Ga)As Double-Heterostructure Lasers: Comparison of Devices Fabricated with Deep and Shallow Proton Bombardment**

By R. W. DIXON and W. B. JOYCE

(Manuscript received November 27, 1979)

*Injection laser light sources must possess improved optical output linearity to be useful in many applications. This paper explores experimentally the optimal linearity and current-threshold distributions of (Al,Ga)As proton-bombardment-delineated, stripe-geometry, double-heterostructure lasers as a function of stripe width and contrasts the cases in which the protons do and do not penetrate the active volume. For comparison, we evaluate the corresponding theoretically expected threshold currents from a new theory of current-crowded carrier confinement. We demonstrate that shallow proton bombardment with adequately narrow stripes can result in satisfactory optical linearity without the threshold penalty that has been associated with narrow-stripe-width devices in which the protons penetrate the active volume.*

### **I. INTRODUCTION**

An important goal of recent injection-laser applied research has been the development of a laser structure that combines the desirable features of good optical linearity, absence of temporal instabilities, high reliability, and a high-yield, simple fabrication process.<sup>1</sup>

With regard to optical linearity, it has been known for some years that controlling the lateral mode motion in stripe-geometry lasers by narrowing the stripe width results in greatly improved linearity of light versus device current (above threshold).<sup>2</sup> However, in proton-bombardment-delineated structures in which the proton damage penetrates the active region of the laser, it has been difficult to narrow the stripe width below about 8  $\mu\text{m}$  without encountering serious increases in lasing current threshold due to excess carrier losses at the stripe edges. This has resulted in the consideration of devices in which the

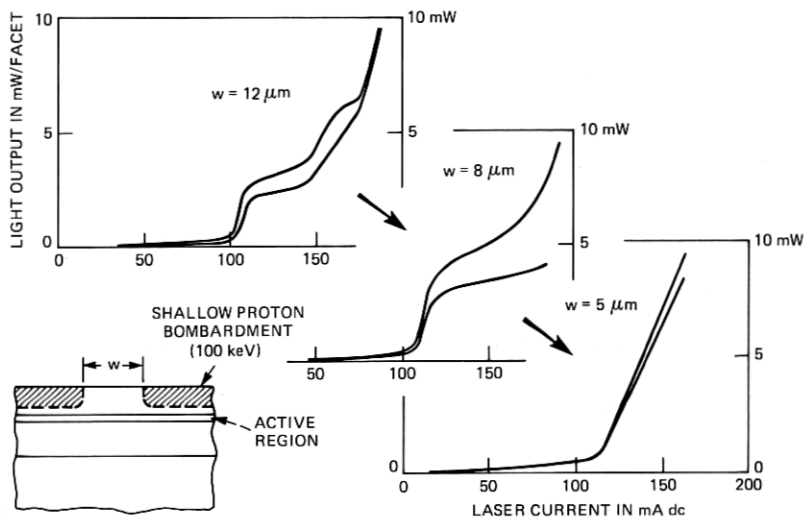


Fig. 1—Light vs current for lasers of varying stripe width ( $w = 12, 8, 5 \mu\text{m}$ ) and shallow proton damage (100 keV).

protons do not penetrate the active volume.<sup>3,4</sup> Also, there has been the considerable concern that proton damage in the active region may adversely impact device reliability. In fact, a statistically meaningful decrease in laser lifetime in 8- $\mu\text{m}$ -stripe-width devices has recently been reported in lasers with median lifetimes at 70°C greater than about 1000 hours.<sup>5</sup>

In this paper, we report the results of investigations into the relationships among threshold current, stripe width, and proton-penetration depth in two wafers of liquid-phase epitaxially grown laser material. The theoretically expected functional dependences among these parameters are also explored, as is the optical linearity above threshold as a function of stripe width. In addition to the experimental results, the present work differs from previous studies<sup>3,4</sup> of shallow-proton lasers in our emphasis, results, and interpretation regarding optical linearity (kink suppression) and in our use of a new theoretical model.

## II. EXPERIMENTAL RESULTS AND QUALITATIVE DISCUSSION

The first set of experimental results to be discussed is shown in Fig. 1. The results in this figure were obtained from measurements on devices that were fabricated from a single wafer of laser material. Devices with stripe widths of 5, 8, and 12  $\mu\text{m}$  were obtained on the same slice by interleaving proton-bombardment masks of these widths. This wafer contained the usual four epitaxial layers, an N- $\text{Al}_{0.36}\text{Ga}_{0.64}\text{As}$  ternary, a p- $\text{Al}_{0.08}\text{Ga}_{0.92}\text{As}$  active region, a P- $\text{Al}_{0.36}\text{Ga}_{0.64}\text{As}$  ternary, and

a p-GaAs final layer. Nominal dimensions and doping levels were as previously reported.<sup>6</sup> The protons used in the device fabrication, however, were accelerated to only 100 keV energies instead of the more common 300 keV. Because of this, they penetrated the wafer only about 0.5  $\mu\text{m}$  and stopped  $\sim 2.0 \mu\text{m}$  short of the active layer.

Figure 1 shows representative light-current curves for the 12-, 8-, and 5- $\mu\text{m}$ -stripe-width devices. Note for the 12- $\mu\text{m}$  case the appearance of kinks at about 2 and 7 mW of optical output per laser facet. Narrowing the stripe width to 8  $\mu\text{m}$  improves the linearity somewhat, but kinking is still severe at about 3 mW; more severe, in fact, than is typically encountered with deeper proton penetration using this stripe width,<sup>2</sup> even if the proton bombardment does not penetrate the active volume. When the stripe width is narrowed further to 5  $\mu\text{m}$ , however, the linearity is significantly improved. The kink now occurs above 8 mW/mirror face. We attribute this improved linearity to the increased gain guiding available in the narrower structure.<sup>1</sup>

Threshold-current comparisons among 30 of the lasers fabricated as described above are shown in Fig. 2. Separate distributions of lasing

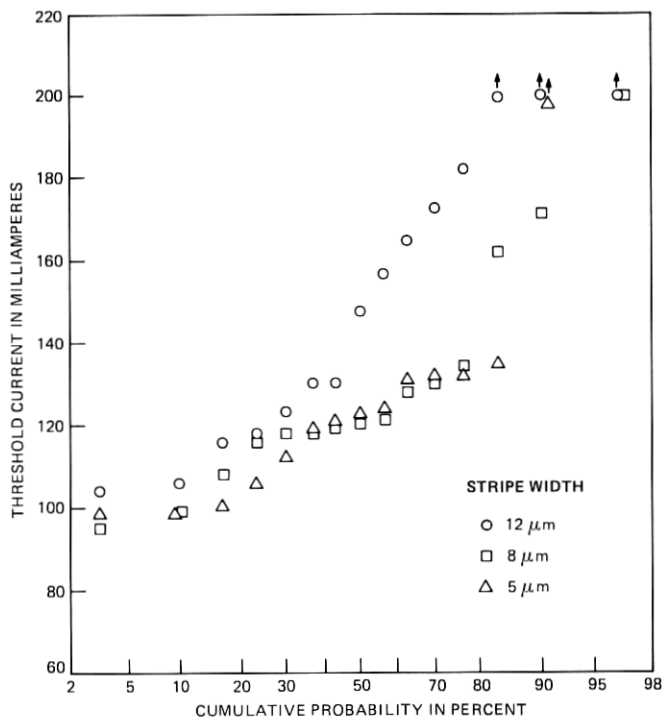


Fig. 2—Steady-state threshold currents for the lasers of Fig. 1 (cumulative probability).

threshold versus cumulative probability (a straight line implies a log-normal distribution) are shown for the 5-, 8-, and 12- $\mu\text{m}$  stripe width devices. Data points with small arrows attached indicate lasers with thresholds above the measurement limit of 200 mA. The important property of shallow bombardment shown in Fig. 2 is that narrowing the stripe width does not increase (and actually slightly decreases) the average laser threshold. This is to be expected, as discussed further below. (However, the current density at the contact, as well as the series resistance, is increased as the stripe is narrowed.)

Experimental results of related experiments performed on another wafer are shown in Fig. 3. In this case, lasers with 5-, 8-, and 12- $\mu\text{m}$  widths were obtained as previously, by interleaving the different-width proton-bombardment masks, but in addition the slice was divided into two parts. One part was bombarded with 300 keV protons, which in general penetrated the active volume, while the other part received 200 keV proton bombardment, which generally stopped  $\sim 0.5 \mu\text{m}$  short of the active volume. A total of 120 lasers, 20 from each category, was measured and the threshold currents are compared in Fig. 3. For the 12- $\mu\text{m}$  stripe width lasers, there is little difference between the threshold distributions in the 300 keV (deep) and 200 keV (shallow) cases. The median thresholds in both cases are about 140 mA. When the stripe width was decreased to 8  $\mu\text{m}$ , the shallow-bombarded lasers, consistent with Fig. 2, showed a decrease in threshold and the deep bombarded lasers showed an increase in threshold. A median difference in threshold of about 40 mA results. When the stripe width was narrowed further to 5  $\mu\text{m}$ , the shallow-threshold distribution changed very little, but the deep-threshold distribution increased substantially so that only one 300 keV device had a threshold below 200 mA. On a subsequent measurement, it was determined that in this device the layer thicknesses were such that in fact the protons had *not* penetrated the active volume. From the data of Fig. 3, we conclude that the substantial threshold penalty, which exists in deep-proton-bombarded lasers as the stripe width is decreased, can be eliminated by using techniques in which the protons do not penetrate the active volume.

### III. THEORETICAL ANALYSIS

As the stripe width is narrowed below 12  $\mu\text{m}$ , the data of Figs. 2 and 3 show that the threshold current increases if the protons penetrate the active region. In contrast, for nonpenetrating protons, the threshold current is seen to decrease somewhat as the contact is narrowed. In a qualitative sense, this behavior is predicted by even the simplest models of laser action, as we now show.

Although solutions are also known<sup>7</sup> for more complex models, we shall, in the absence of better data, make the simplest possible choice

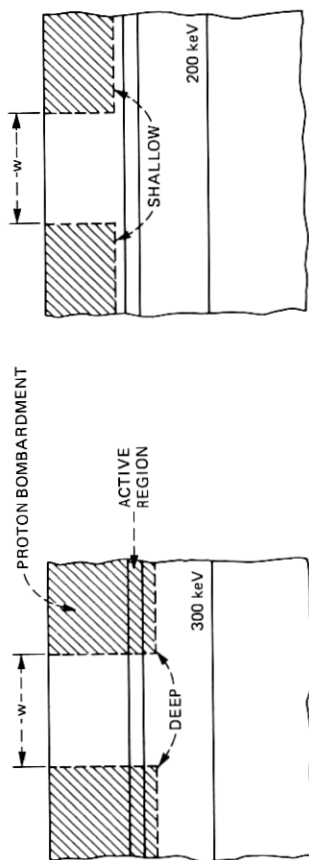
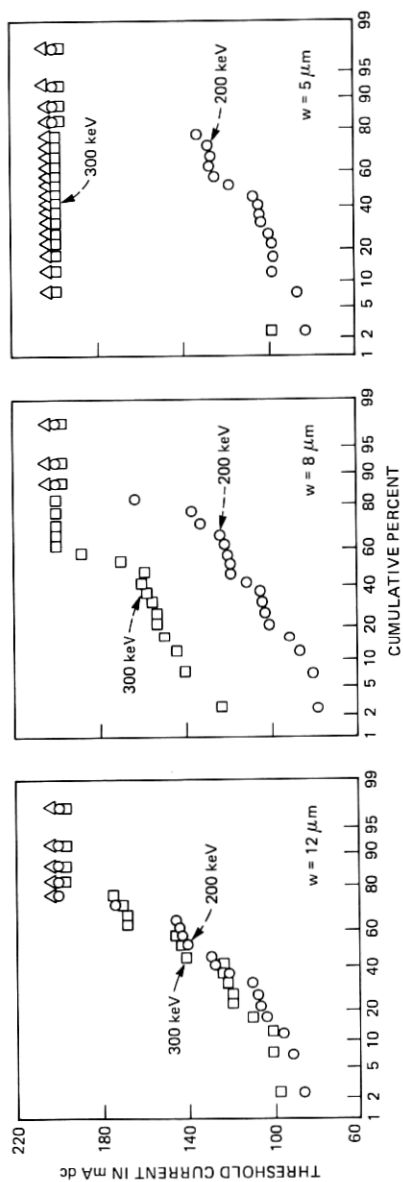
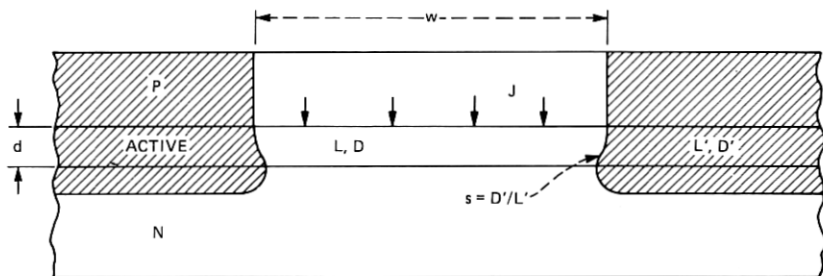
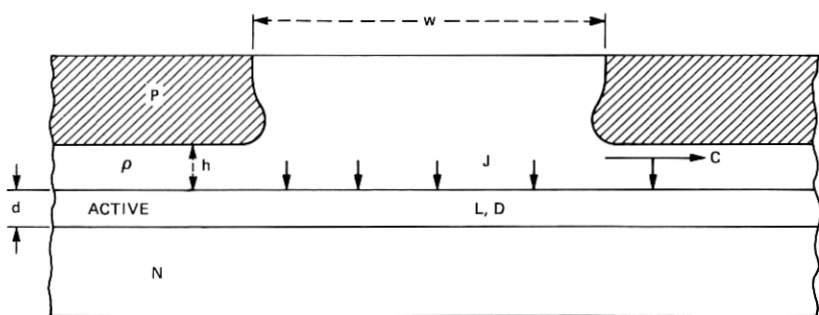


Fig. 3.—Steady-state threshold currents for lasers of varying stripe width ( $w = 12, 8, 5 \mu\text{m}$ ) with active-region penetrating (300 keV) and nonpenetrating (200 keV) proton damage.



(a)



(b)

Fig. 4—Current flow for (a) active-region penetrating and (b) nonpenetrating proton damage.

and assume that the low-doped active region can be characterized by constant values of the carrier diffusion length  $L = (D\tau)^{1/2}$ , lifetime  $\tau$ , and diffusion coefficient  $D$ . The part of the active layer beyond the stripe, if proton bombarded, acquires new constant values  $D'$  and  $L'$  and thus appears to the unbombarded part of the active layer as a surface of recombination velocity  $s = D'/L'$  (Fig. 4a). For proton bombardment which penetrates the active region, the (assumed-uniform) junction-current density  $J$  ( $A/cm^2$ ) and the circuit current  $I$  ( $A$ ) are given by<sup>7-9</sup>

$$I = wJ = n_0(1 - 1/y)^{-1}wlqDd/L^2 \quad (1)$$

$$\rightarrow 2n_0sqld, \quad w \rightarrow 0, \quad (2)$$

where

$$y = \cosh(w/2L) + (D/Ls)\sinh(w/2L). \quad (3)$$

To evaluate eq. (1), we take from the work of Nelson and Rode<sup>10</sup> the experimentally based values  $s = 7 \times 10^5$  cm/s and  $D = 33$  cm<sup>2</sup>/s for a

typical 100-mA threshold laser with  $d = 0.15 \mu\text{m}$ ,  $w = 12 \mu\text{m}$ , and laser length  $l = 380 \mu\text{m}$ . If it is assumed that the threshold carrier concentration at the stripe center is  $n_0 = 1.5 \times 10^{18} \text{cm}^{-3}$ , eq. (1) then yields  $L = 2.535 \mu\text{m}$  and, hence,  $\tau = L^2/D = 1.95 \text{ns}$ . Equation (1) appears as the "protons-penetrate-active" curve in Fig. 5a.

If the protons fall short of the active layer and leave a thickness  $h$  of the P layer with its original unbombarded resistivity  $\rho = 0.24 \Omega\text{-cm}$ , then the threshold current  $I$  includes not only the current  $wlJ$  injected under the contact, but also the current  $IC$  escaping within the P layer from each side of the stripe (Fig. 4b); i.e.

$$I = wlJ + 2IC. \quad (4)$$

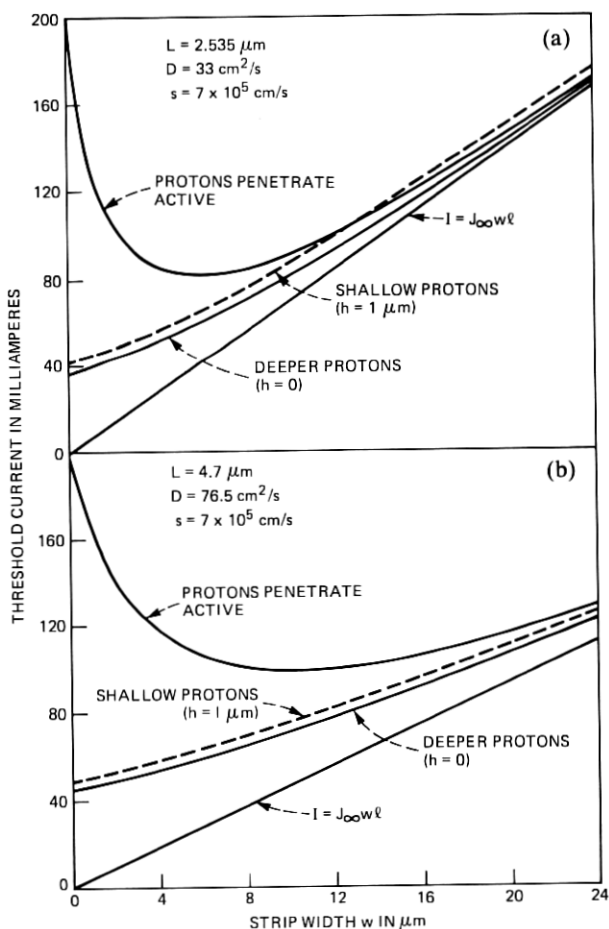


Fig. 5—Theoretical threshold current vs stripe width. (a) Short diffusion length ( $L = 2.5 \mu\text{m}$ ). (b) Long diffusion length ( $L = 4.7 \mu\text{m}$ ).

Compensating, indeed usually more than compensating, for the leakage current  $2IC$  added by the retraction of the protons is the reduction in  $s$  to its unbombarded value  $s = D/L = 1.3 \times 10^5$  cm/s.  $J$  and  $C$  are conveniently evaluated in terms of the carrier concentration  $n_e$  at the stripe edge ( $x = w/2$ ) as<sup>7</sup>

$$J = [n_0 + fL/\sinh(w/2L)]qDd/L^2 \quad (5)$$

$$C = fzqDd, \quad (6)$$

where

$$z = 2kTh/q^2\rho Dn_e d \quad (7)$$

$$f = (n_e/L)(1 + 2z)^{1/2}(1 + z)^{-1}. \quad (8)$$

The relation between  $n_e$  and  $n_0$  is<sup>7</sup>

$$n_0 = n_e + fL[\cosh(w/2L) - 1]/\sinh(w/2L). \quad (9)$$

Equation (4) is plotted in Fig. 5a for the case of shallow protons ( $h = 1 \mu\text{m}$ ) and for deeper protons which nearly reach the active layer ( $h \rightarrow 0$ ).

If there were no loss of carriers at the stripe edge, the threshold would fall to the value

$$I = J_\infty wl, \quad (10)$$

where  $J_\infty = qn_0d/\tau$  is the broad-area threshold current density.

Alternately, we consider the consequences of the longer diffusion lengths reported by Hakki<sup>9</sup> by taking as a typical case  $L = 4.7 \mu\text{m}$ . Retention of the values  $s = 7 \times 10^5$  cm/s,  $d = 0.15 \mu\text{m}$ ,  $l = 380 \mu\text{m}$ ,  $w = 12 \mu\text{m}$ ,  $T = 300\text{K}$ , and  $n_0 = 1.5 \times 10^{18}$  cm<sup>-3</sup> implies that, in a 100-mA-threshold laser with penetrating protons, the new parameter values are  $D = 76.5$  cm<sup>2</sup>/s and  $\tau = 2.89$  ns. The new family of curves is shown in Fig. 5b.

In a qualitative way, both forms of Fig. 5 capture the typical experimental trends—an optimum (minimum-threshold) stripe width for penetrating protons but an ever-decreasing threshold for non-penetrating protons. According to the new theory of current crowding which we utilize, relatively little current is lost in the P layer because the outdiffusion of carriers in the active layer suppresses injection from those parts of the P layer outside of the stripe.<sup>7</sup> Figure 5a better represents the small observed threshold difference between penetrating and nonpenetrating protons at  $w = 12 \mu\text{m}$ . Figure 5b better represents the observed rapid threshold increase with stripe narrowing in the case of penetrating protons.

Although the qualitative trends seen in Fig. 5 are consistent with the data in Figs. 1 to 3, accurate quantitative agreement could not be



obtained for any choice of parameters which we considered reasonable. Factors not incorporated in such simple models are apparently too important to be absorbed into effective parameter values. These factors may include nonconstant  $D$ ,  $L$ , and  $\tau$  (see Ref. 7), carrier drift in the active layer,  $w$ -dependent optical loss, heating, changing ratio of average modal gain to center-line gain, inadvertently inequivalent processing of lasers with different proton dosage, and escape of injected carriers into the confining ternary layers.

It should be emphasized that the optimum (threshold-minimizing) stripe width for deep-proton-bombarded lasers is not a very fundamental or consistent quantity. Experimentally, we have seen this variability and, in fact, the threshold difference between 12- $\mu\text{m}$  and 8- $\mu\text{m}$  lasers shown in Fig. 3 is larger than we have often observed in other stripe-width comparisons such as that described in Ref. 2. There are a number of theoretical reasons for expecting this variability, including the following: Slice-to-slice variations in the diffusion length  $L$  shift the optimum width significantly. (The optimum width is shifted from  $\sim 6 \mu\text{m}$  to  $\sim 10 \mu\text{m}$  in Fig. 5 as  $L$  is changed from  $2.5 \mu\text{m}$  to  $4.7 \mu\text{m}$ .) The surface-recombination velocity  $s$  is reduced dramatically with annealing,<sup>10</sup> and thus the optimum width varies with intentional and inadvertent temperature-cycle variations during processing and perhaps even during device operation. As suggested by the straggler-bulge in the proton-edge contour in Fig. 4a, there can also be a significant difference between the nominal stripe width  $w$  and the effective width in the active region. This difference would, for example, vary with slice-to-slice variations in the P-layer thickness. In contrast, the shallow-bombarded laser has the advantage that its threshold is a much less critical function of the stripe width.

Many theoretical explanations of the light-current kink have been published. Most appear to be incorrect either because they assumed structural asymmetry or else because they considered only gain guiding or only symmetric (undisplaced) modes. The essentially correct explanation, we believe, is due to Thompson et al.<sup>1,11</sup> In that theory, the kink occurs when the real-refractive-index guiding (which arises from spatial hole burning) overcomes the gain guiding and causes the observed<sup>2</sup> lateral mode displacement. An indicator of the resistance to kinking is thus the centerline concentration curvature  $-d^2n_0/dx^2$ , which is the controlling parameter in the theory of gain guiding.<sup>12</sup> From the previously developed formula,<sup>7</sup>

$$-d^2n_0/dx^2 = J/qDd - n_0/L^2, \quad (11)$$

the curvature is plotted in Fig. 6 as a function of the stripe width. We attribute the kink resistance of narrow-stripe lasers primarily to the dramatic increase in curvature which results from stripe narrowing.

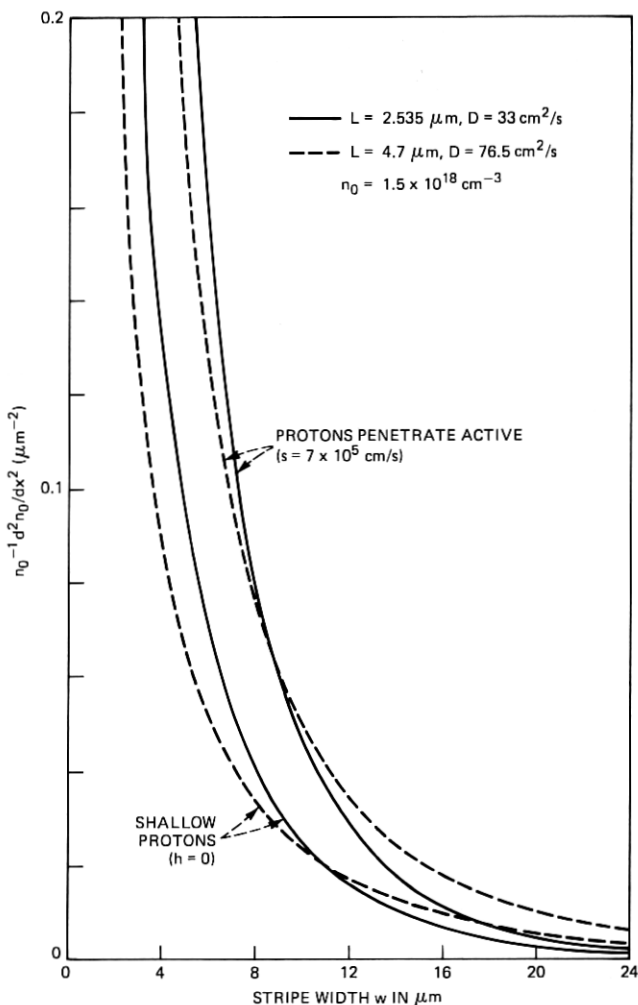


Fig. 6—Theoretical concentration curvature at threshold vs stripe width.

Similarly, protons which penetrate the active region produce more curvature than do shallower protons. This is consistent with our observation that the kink occurs at higher optical power, for a given stripe width, when the protons penetrate. (On the other hand, the curvature is fairly insensitive to the proton depth when the protons come reasonably close to, but do not enter, the active region, and only the  $h = 0$  case is shown in Fig. 6.) Because shallow protons produce less curvature, the width over which current is injected into the active region in these devices must therefore be relatively narrow. The importance of this increases in current density at the contact and in

differential device impedance implied by this, including any adverse impact on reliability, remains to be investigated.

#### IV. SUMMARY AND CONCLUSION

GaAs stripe-geometry lasers fabricated from slices in which proton-delineated stripe widths of 12, 8, and 5  $\mu\text{m}$  were alternated have been investigated. Shallow proton bombardment, in which protons do not penetrate the active volume, has also been compared with the case of deeper bombardment. The results suggest that lasers with shallow bombardment and narrow stripes can have adequate optical linearity and improved lasing threshold distribution. We also find that fabricating these devices with half-wavelength coatings of  $\text{Al}_2\text{O}_3$  stabilizes their pulsation characteristics, as was predicted<sup>13</sup> and verified experimentally<sup>14</sup> for more deeply bombarded devices.

#### V. ACKNOWLEDGMENTS

It is a pleasure to acknowledge the assistance of N. E. Schumaker, B. Schwartz, and L. A. Koszi in the growth and fabrication of the devices discussed here.

#### REFERENCES

1. R. W. Dixon, "Current Directions in GaAs Laser Device Development," B.S.T.J., 59, No. 5 (May-June 1980), pp. 669-722.
2. R. W. Dixon, F. R. Nash, R. L. Hartman, and R. T. Hepplewhite, Appl. Phys. Lett., 29 (1976), p. 372.
3. A. G. Steventon, P. J. Fiddymont, and D. H. Newman, Optical and Quantum Electronics, 9 (1977), p. 519.
4. J. C. Bouley, Ph. Delpuch, J. Charl, G. Chaminant, J. Landreau, and J. P. Noblanc, Appl. Phys. Lett., 33 (1978), p. 327.
5. R. L. Hartman and R. W. Dixon, J. Appl. Phys., to be published.
6. W. B. Joyce and R. W. Dixon, J. Appl. Phys., 46 (1975), p. 255.
7. W. B. Joyce, J. Appl. Phys., 51 (1980), p. 2394.
8. A. Many, Y. Goldstein, and N. B. Grover, *Semiconductor Surfaces*, Amsterdam: North Holland, 1965, eq. 17.4.
9. B. W. Hakki, J. Appl. Phys., 44 (1973), p. 5021.
10. R. J. Nelson and D. L. Rode, J. Appl. Phys., 50 (1979), p. 5135.
11. G. H. B. Thompson, D. F. Lovelace, and S. E. H. Turley, Solid-State and Electron Devices, 2 (1978), p. 12.
12. F. R. Nash, J. Appl. Phys., 44 (1973), p. 4696.
13. R. W. Dixon and W. B. Joyce, IEEE J. Quant. Elect., QE-15 (1979), p. 470.
14. F. R. Nash, R. L. Hartman, T. L. Paoli, and R. W. Dixon, Appl. Phys. Lett., 35 (1979), p. 905.

